Supplementary Material

Supplementary Figure Legends

Figure S1. Thermal melting curves for Bcl-x_L and RX1 monitored by mean residue ellipticity at 222 nm. Experimental conditions are described in Materials and Methods.

Figure S2. Fluorescence polarization experiments and fitted curves characterizing binding of Bcl-x_L and RX1 to fluorescently labeled Bim or Bad BH3 peptides. The different dye-labeled peptides used are indicated on each plot and described in Table S3. The average values as well as the standard deviation of two independent measurements of anisotropy are plotted as a function of Bcl-x_L/RX1 concentration. Fitted values are listed in Table S4. Experimental conditions and curve fitting for the direct binding experiments are described in Materials and Methods.

Figure S3. Fluorescence polarization experiments and fitted curves characterizing binding of Bcl-x_L and RX1 point mutants to fluorescently labeled Bad BH3 peptides, presented as in Figure S2.

Figure S4. Fluorescence polarization experiments and fitted curves characterizing binding of Bcl-x_L, RX1 and different Bcl- x_L point mutants to unlabeled Bim-22 (open diamond) or Bad-22 (closed circle) peptides by competition. The Bcl-x_L variant, the competitor peptide, and the fluorescently labeled peptide being competed off are indicated on each plot. The average values as well as the standard deviation of two independent measurements are plotted as a function of competitor peptide concentration. Fitted values are listed in Table S6. Experimental conditions and curve fitting for these competition experiments are described in Materials and Methods.

Figure S5. Fluorescence polarization experiments and fitted curves characterizing binding of different RX1 point mutants to unlabeled Bim-28 (open diamond) or Bad-28/Bad-22 (closed circle) peptides by competition, presented as in Figure S4. Fitted values are listed in Table S7.

Figure S6. The influence of point mutations in RX1 on binding to Bim or Bad BH3, using the Bim-26 and Bad-26 (for RX1 mutants L105F, I122S, V125Q, G142A) or Bad-22 (for RX1 mutants H101Y, G111Q, A126V, I130L, A146F) peptides. (A) Fluorescence polarization experiments and fitted curves characterizing binding of Bcl-x_L, RX1 and different RX1 point mutants to unlabeled Bim-26 (open diamond) or Bad-26/Bad-22 (closed circle) peptides by competition, presented as in Figure S4. Fitted values are listed in Table S7. (B) Ratios of the K_i values for Bcl-x_L point mutants binding Bim (white) or Bad (gray) to the K_i values for Bcl-x_L binding the same BH3 peptide are shown. Peptide sequences are given in Table S3.

Figure S7. Fluorescence polarization experiments and fitted curves characterizing binding of Bcl-x_L (open diamond), RX1 (closed circle) to unlabeled Bad mutant peptides by competition. The fBad-23 peptide was competed off in all experiments. The competitor peptide is indicated on each plot. The average values as well as the standard deviation of two independent measurements are plotted as a function of competitor peptide concentration. Fitted K_i values for Bcl-x_L and RX1 interacting with different BH3 peptides are listed in Table S8. Experimental conditions and curve fitting for these competition experiments are described in Materials and Methods.

Figure S8. Sites of mutations modeled on crystal structures of the Bcl-x_L/Bad complex (PDB ID: 2BZW). (A) The interface between Bcl-x_L and a Bad BH3 peptide (PDB ID: 2BZW), with Bcl-x_L in cyan and the peptide shown as green sticks. Positions mutated in RX1 are in blue. (B) Interaction between A142 of Bcl-x_L and S3e of Bad, as shown in the crystal structure between mouse Bcl-x_L (cyan) and Bad (green) (PDB ID: 2BZW). In RX1, A142 was mutated to Gly. The 3e position is occupied by Gly for Bim, and Ala for PUMA. (C) Possible coupling between F146 and the α3 helix of Bcl-x_L through Y2d of Bad. Structural alignment of Bcl-x_L/Bad (PDB ID: 2BZW, shown in magenta) and Bcl-x_L/Bim (PDB ID: 3FDL, shown in yellow) illustrate the different conformations of the α3 helices in the two structures. Images generated using PyMol (Delano Scientific).

Supplementary Tables

Table S1. Unique sequences isolated from the first designed library

	F97	Y101	A104	L108	L112	V126	E129	L130	A142	Other[b]	#[c]
A2	F	H[a]	W	R	L	V	I	I	G		1
A3	F	Y	A	L	M	A	V	L	G		1
A4	F	H	F	A	L	A	A	L	G		1
B2	F	H	F	T	L	V	T	I	G	Q111K	7
B4	F	Y	A	V	V	A	E	V	G		1
B5	F	Y	M	L	L	A	V	L	G		1
C1	F	Y	M	V	L	A	E	I	G		1
C3	F	H	W	S	L	V	T	I	G		1
C4	F	H	F	T	L	V	V	I	G		1
C5	F	H	K	L	L	A	I	L	G	S122I	1
C6	L	H	F	R	L	V	T	I	G		1
D3	F	H	A	L	L	T	V	L	G		1
D5	F	H	W	R	L	I	E	I	G		1
D6	F	H	F	T	L	V	T	I	G		1
E2	F	Y	M	V	L	S	E	I	G		1
E5	F	H	W	R	L	I	T	I	G		2
F4	F	Y	A	V	L	A	E	I	G		1
G3	F	H	F	R	L	T	V	L	G		1
G5	F	H	F	T	L	A	E	L	G		1
H3	F	H	W	R	L	A	E	L	G		1
H6	F	H	M	T	L	V	V	L	G	R103W	1

[a] Shaded mutations were either not included in the modeling or not predicted as "non-disruptive" residues, but were included in the library due to degenerate codons.
[b] Mutations under the "other" column were not included in the library design.
[c] Number of clones recovered with this sequence.

Table S2. Unique sequences of specific binders isolated from the second designed library after two sorts [a]

	E96	Y101	A104	L108	Q111	S122	Q125	V126	E129	L130	F146	Y195	Other	#[b]
A1	Q	H	M	L	D	V	V	V	E	I	A	Y		1
A3	L	H	A	L	G	I	I	A	E	L	A	Y		1
A4	Q	H	A	L	E	V	I	A	V	L	A	F		1
A5	L	H	A	L	S	L	I	A	E	L	A	Y		1
B1	L	H	M	L	E	F	I	A	E	L	A	Y		1
B3	Q	H	A	L	T	I	L	A	E	L	A	Y		1
B4	Q	H	A	L	S	V	I	V	E	I	A	Y		1
B6	R	H	A	L	S	V	T	A	E	L	A	Y		1
C2	V	H	A	L	T	I	I	A	E	L	A	Y		1
C6	V	H	A	L	Q	I	E	A	E	L	A	Y		1
D2	Q	H	A	L	D	V	V	V	E	I	A	Y		2
D4	Q	H	A	L	D	I	I	V	E	I	A	Y	A85T	1
D5	G	H	A	L	S	V	V	A	E	L	A	Y		1
E2	L	H	A	L	P	I	I	V	E	I	A	Y	F105I	1
E3	G	H	A	L	E	V	I	A	V	L	A	F		1
E4	Q	Y	M	L	E	I	I	A	E	I	A	Y		1
E6	Q	H	A	L	L	F	I	A	E	I	A	Y		1
F1	L	H	A	L	Q	I	V	V	E	I	A	Y		1
F2	E	H	M	L	E	V	I	V	E	I	A	Y		1
F3	R	H	A	L	T	T	I	A	E	L	A	Y		1
F4	R	H	A	L	H	V	V	A	E	L	A	Y		2
F5	L	H	A	L	S	I	E	A	E	L	A	Y		1
G2	L	H	A	L	D	T	E	A	E	L	A	Y	F105L	1
G3	L	H	M	L	E	F	I	A	E	L	A	Y		1
G5	Q	H	M	L	D	T	A	A	E	L	A	Y	F105L	1
G6	L	H	A	L	G	L	I	A	E	L	A	Y		1
H3	Q	H	M	L	N	I	V	A	E	L	A	Y		1
H5	Q	H	M	L	N	I	I	A	E	L	A	Y		1

[a] See descriptions for Table S1. The shaded Pro is the only mutation that was not predicted as non-disruptive. Note that, relative to Bcl-x_L, all variants also had mutation A142G, identified in library 1 screening.

[b] Number of clones recovered with this sequence.

Table S3. BH3 peptides used in this study

	2------3------4------ efgabcdefgabcdefgabcdefgab	Origin[a]
Bim-28	MRPEIWIAQELRRIGDEFNAYYARRVFL	recombinant
Bad-28	LWAAQRYGRELRRMSDEFVDSFKKGLPR	recombinant
Bim-26	MRPEIWIAQELRRIGDEFNAYYARRV	synthetic
Bad-26	LWAAQRYGRELRRMSDEFVDSFKKGL	synthetic
Bim-22	MRPEIWIAQELRRIGDEFNAYY	synthetic
Bad-22	LWAAQRYGRELRRMSDEFVDSF	synthetic
Bad-22-G2eL	LWAAQRYLRELRRMSDEFVDSF	synthetic
Bad-22-L3aD	LWAAQRYGREDRRMSDEFVDSF	synthetic
Bad-22-S3eL	LWAAQRYGRELRRMLDEFVDSF	synthetic
Bad-22-D3fK	LWAAQRYGRELRRMSKEFVDSF	synthetic
Bad-22-F4aE	LWAAQRYGRELRRMSDEEVDSF	synthetic
Bak	SSTMGQVGRQLAIIGDDINRRYDSEFQT	recombinant
Bax	DASTKKLSECLKRIGDELDSNMELQRMI	recombinant
Beclin	GGTMENLSRRLKVTGDLFDIMSGQTDVD	recombinant
Bid	EDIIRNIARHLAQVGDSMDRSIPPGLVN	recombinant
Bik	MEGSDALALRLACIGDEMDVSLRAPRLA	recombinant
Bmf	HQAEVQIARKLQCIADQFHRLHVQQHQQ	recombinant
Hrk	SSAAQLTAARLKALGDELHQRTMWRRRA	recombinant
Mule	GVMTQEVGQLLQDMGDDVYQQYRSLTRQ	recombinant
Noxa	AELEVECATQLRRFGDKLNFRQKLLNLI	recombinant
Puma	EQWAREIGAQLRRMADDLNAQYERRRQE	recombinant
fBad-21[b,c]	NLWAAQRYGRELRRMSDKFVD	synthetic
fBad-23[b]	Fl-NLWAAQRYGRELRRMSDEFVDSF	synthetic
fBad-27[b]	Fl-NLWAAQRYGRELRRMSDEFVDSFKKGL	synthetic
fBim-27[b]	Fl-DMRPEIWIAQELRRIGDEFNAYYARRV	synthetic

-

[a]Recombinant peptides all have an N-terminal His tag followed by a 12-residue long linker, and a C-terminal Flag tag preceded by a GlyGly 2-residue long linker. The complete sequence for a recombinant BH3 peptide is: SHHHHHHGESKEYKKGSGS-BH3 peptide-GGDYKDDDDK.

[b]F1 stands for FITC.

[c]The FITC label is on the underlined Lys residue

Table S4. Fitted K_d values for direct binding experiments between Bcl-x_L variants and different fluorescently labeled peptides (fitted curves shown in Fig. S3, S4). Methods for obtaining the average and standard deviation for each K_d value are described in Materials and Methods.

	Labeled peptide	K_d (nM)
Bcl-x_L	fBad-23	3.3±0.4
	fBim-27	< 1
	fBad-27	< 1
RX1	fBad-23	22±4
	fBim-27	3,800±400
	fBad-27	1.7±0.2
Y101H	fBad-23	23±5
A104M	fBad-21	3.8±0.5
F105L	fBad-23	8.9±3.5
Q111G	fBad-23	6.4±2.0
S122I	fBad-21	4.2±0.1
Q125V	fBad-21	4.7±2.0
V126A	fBad-23	16±3
L130I	fBad-23	31±3
A142G	fBad-21	1.6±0.3
F146A	fBad-23	63±14
RX1-H101Y	fBad-23	2.9±0.7
RX1-L105F	fBad-27	6.8±1.6
RX1-G111Q	fBad-23	13±1
RX1-I122S	fBad-27	40±8
RX1-V125Q	fBad-27	17±5
RX1-A126V	fBad-23	17±3
RX1-I130L	fBad-23	3.6±0.4
RX1-G142A	fBad-27	35±8
RX1-A146F	fBad-23	21±1

Table S5. Fitted K_i values (nM) for Bcl-x_L and RX1 interacting with different BH3 peptides. Methods for obtaining the average and standard deviation for each K_i value are described in Materials and Methods.

	Bcl-x_L	RX1
Bad-28	<0.1	0.26±0.07
Bim-28	<0.1	2,300±400
PUMA	<0.1	35±8
Bid	34±5	>20,000
Bak	11±3	>20,000
Bax	200±30	>20,000
Bmf	0.25±0.15	>20,000
Bik	26±7	>20,000
Hrk	0.17±0.05	>20,000
Beclin	>1,000	>20,000
MULE	>1,000	>20,000
Noxa	>1,000	>20,000

Table S6. Fitted K_i values (nM) for point mutants of Bcl-x_L binding Bim or Bad BH3. Methods for obtaining the average and standard deviation for each K_i value are described in Materials and Methods.

	Bim-22	Bad-22
Bcl-x_L	3.4±1.4	1.8±0.6
RX1	>50,000	33±5
Bcl-x_L-Y101H	10±2	25±9
Bcl-x_L-A104M	2.3±0.4	0.44±0.08
Bcl-x_L-F105L	4.6±3.2	8.6±3.1
Bcl-x_L-Q111G	2.0±0.9	11±4
Bcl-x_L-S122I	1.3±0.2	0.17±0.01
Bcl-x_L-Q125V	0.68±0.31	0.40±0.24
Bcl-x_L-V126A	110±60	20±6
Bcl-x_L-L130I	27±7	38±14
Bcl-x_L-A142G	2.7±0.8	0.16±0.04
Bcl-x_L-F146A	77±19	70±30

Table S7. Fitted K_i values (nM) for point mutants of design RX1 binding Bim or Bad BH3. Methods for obtaining the average and standard deviation for each K_i value are described in Materials and Methods.

	Bad-22	Bad-28	Bim-28	Bad-26	Bim-26
RX1	33±5	0.26±0.07	2,300±400[a]	0.97±0.18	1,400±200
RX1-H101Y	4.1±1.5	-	200±50[a]	-	110±30
RX1-L105F	-	1.3±0.7	1,600±300[a]	6.4±1.4	850±190
RX1-G111Q	17±2	-	1,500±200[a]	-	800±70
RX1-I122S	-	7.1±2.8	3,400±800[a]	52±18	1,700±600
RX1-V125Q	-	4.0±2.7	>8,000[a]	18±14	11,000±4000
RX1-A126V	34±5	-	310±70	-	360±90
RX1-I130L	6.0±1.2	-	290±40[a]	-	230±60
RX1-G142A	-	8.0±5.0	440±150	34±5	500±130
RX1-A146F	39±2	-	130±10	-	150±20

[a]Limited solubility of Bim-28 at high concentration prevented accurate determination of the lower baseline when fitting dissociation constants. Fitted values were obtained by imposing a lower baseline as described in *SI text*.

Table S8. Fitted K_i values (nM) for Bcl-xL and RX1 interacting with different Bad mutants[a]. Methods for obtaining the average and standard deviation for each K_i value are described in Materials and Methods.

	Bcl-xL	RX1
Bad-22	1.8±0.6	33±5
Bad-22-G2eL	>1,000	>20,000
Bad-22-L3aD	>1,000	>20,000
Bad-22-S3eL	>1,000	4,600±500
Bad-22-D3fK	330±40	5,000±900
Bad-22-F4aE	>1,000	5,200±1,200

[a] Inhibition did not reach completion even at the highest peptide concentration and fitted values were obtained by imposing a lower baseline as described in *SI text*.

Table S9. Oligonucleotides introducing randomization

	Oligonucleotides	Positions randomized
1st library	5'-GCTGTCCCTGGGGTGATGTGCAHCTGGGATGTAVBGTCA CTGAAMNHCCGCCGAWRCCGCAGTTCMAWCTCGTCGCCTG CCTCCCTC-3' (reverse)	F97, Y101, A104, L108, L112
	5'-CACATCACCCCAGGGACAGCATATCAGAGCTTTGAACAG RBKGTGAATRHAVTCTTCCGGGATGGGGTAAACTGG-3'	V126, E129, L130
	5'-TTCCGGGATGGGGTAAACTGGGGTCGCATTGTGRSCTTTT TCTCCTTCGGCGGGGCAC-3'	A142
2nd library	5'-CTGTCCCTGGGGTGATGTGCAAMNBGGATGTCASGTCACT GAATGCCCGCCGATRCCGCAGTTCAAATHSGTCGCCTGCCTC CCTCAGC-3' (reverse)	E96, Y101, A104, L108, Q111
	5'-CTGTCCCTGGGGTGATGTGCAAMNBGGATGTCASGTCACT GAACATCCGCCGATRCCGCAGTTCAAATHSGTCGCCTGCCTC CCTCAGC-3' (reverse)	
	5'-CGACCCCAGTTTACACCGTCCCGGAAGAKTWCATTCACT RCADHTTCAAAGDNCTGATATGCTGTCCCTGGGGTGATGTG CAA-3' (reverse)	S122, Q125, V126, E129, L130
	5'-CGACCCCAGTTTACACCGTCCCGGAAGAKTWCATTCACT RCTHSTTCAAAGDNCTGATATGCTGTCCCTGGGGTGATGTG CAA-3' (reverse)	
	5'-CTTCCGGGACGGTGTAAACTGGGGTCGCATTGTGGGCTTT TTCTCCTTSGGCGGGGCACTGTGCGTGG-3'	F146
	5'-CTTCCGGGACGGTGTAAACTGGGGTCGCATTGTGGGCTTT TTCTCCGCTGGCGGGGCACTGTGCGTGG-3'	
	5'-CTCTCGGCTGCTGCATTGTTCCCGWAGAGTTCCACAAAAG TATCCCAGC-3' (reverse)	Y195

Figure S1

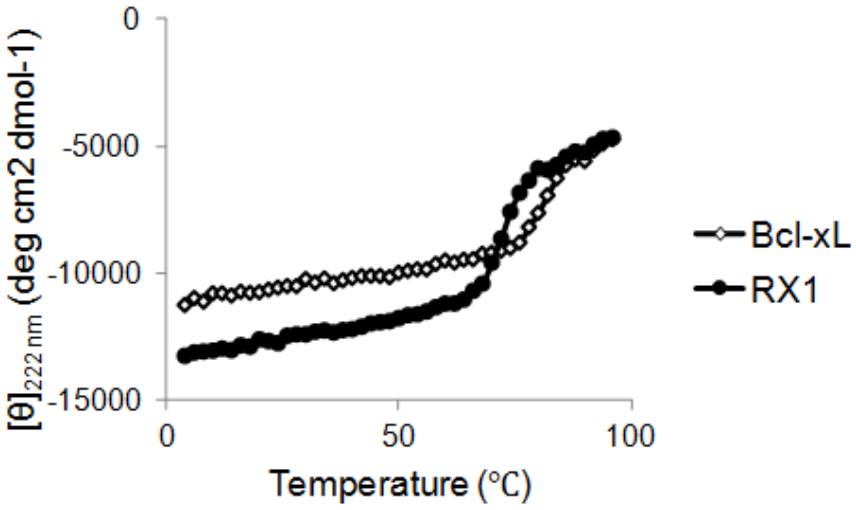
0
-5000
-10000
-15000
[θ]222 nm (deg cm2 dmol-1)
0
50
100
Temperature (°C)
Bcl-xL
RX1

Figure S2

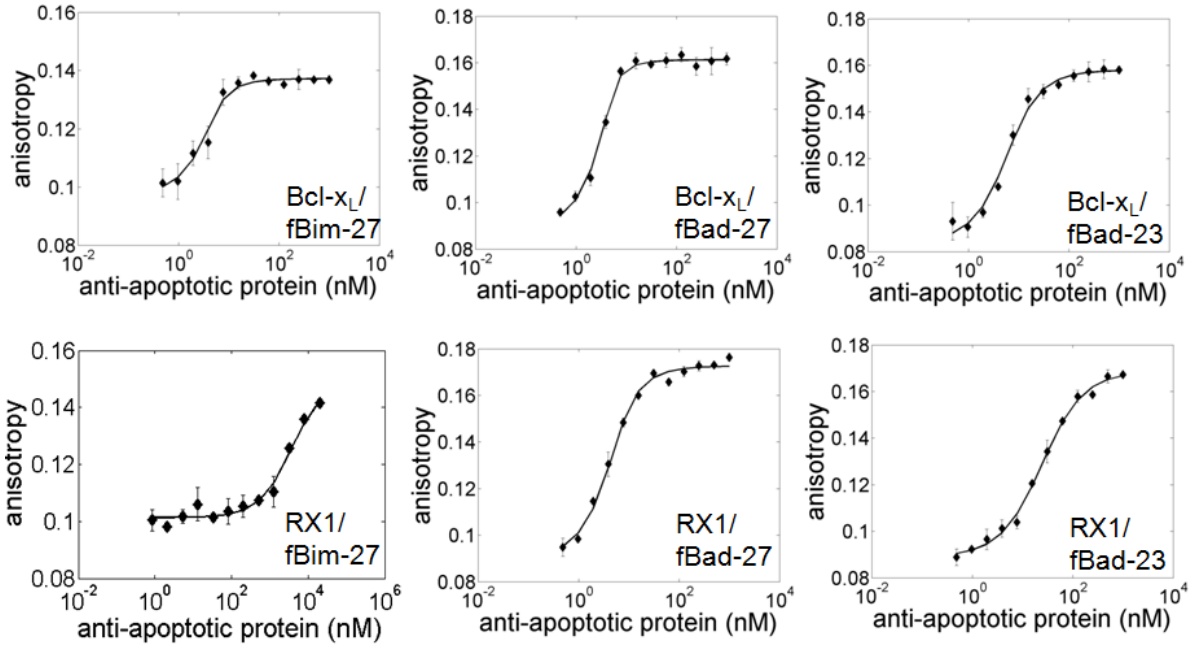
anisotropy
anti-apoptotic protein (nM)
Bcl-x$_L$/ fBim-27
Bcl-x$_L$/ fBad-27
Bcl-x$_L$/ fBad-23
RX1/ fBim-27
RX1/ fBad-27
RX1/ fBad-23

Figure S3

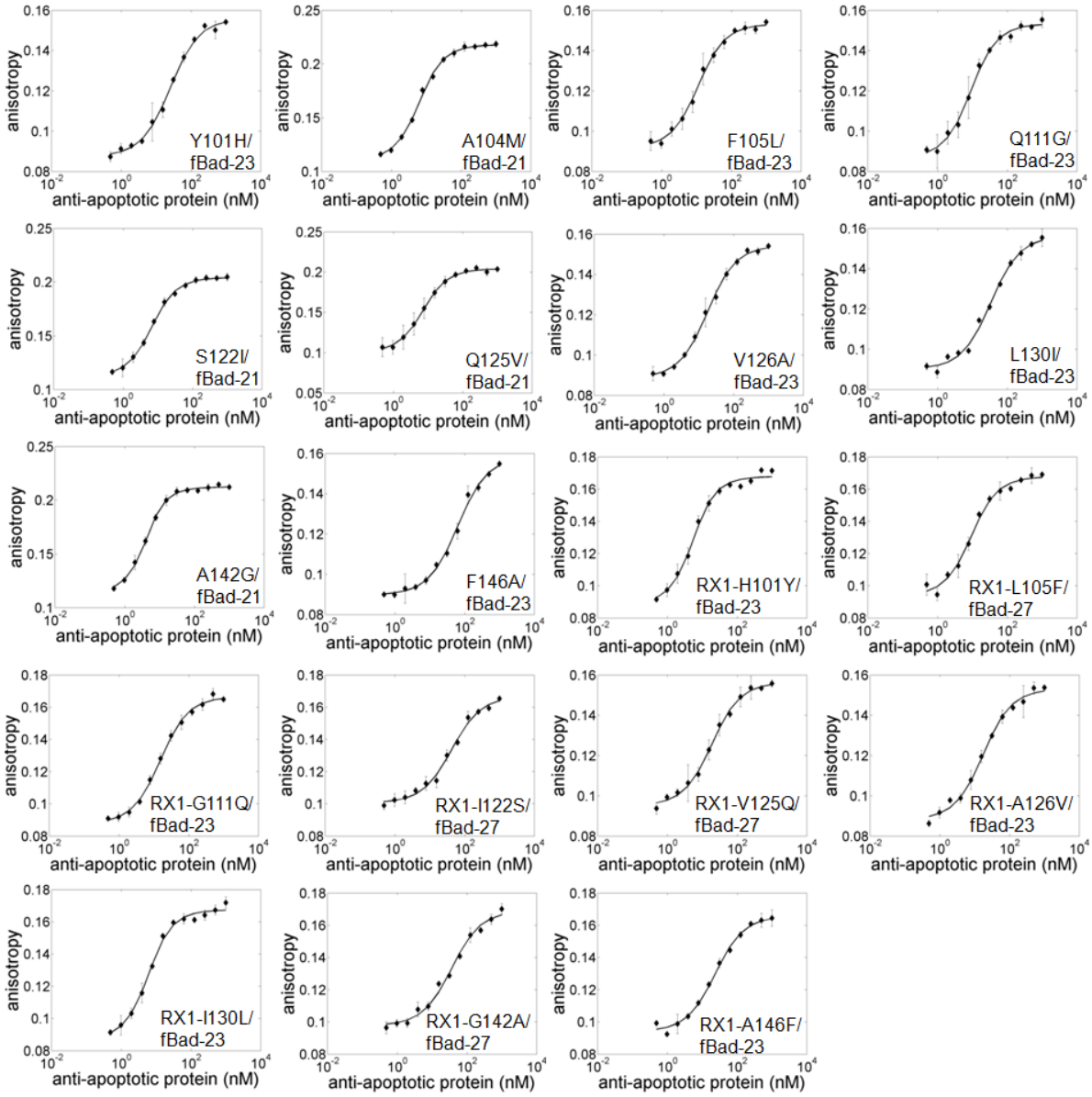
anisotropy
anti-apoptotic protein (nM)
Y101H/ fBad-23
A104M/ fBad-21
F105L/ fBad-23
Q111G/ fBad-23
S122I/ fBad-21
Q125V/ fBad-21
V126A/ fBad-23
L130I/ fBad-23
A142G/ fBad-21
F146A/ fBad-23
RX1-H101Y/ fBad-23
RX1-L105F/ fBad-27
RX1-G111Q/ fBad-23
RX1-I122S/ fBad-27
RX1-V125Q/ fBad-27
RX1-A126V/ fBad-23
RX1-I130L/ fBad-23
RX1-G142A/ fBad-27
RX1-A146F/ fBad-23

Figure S4

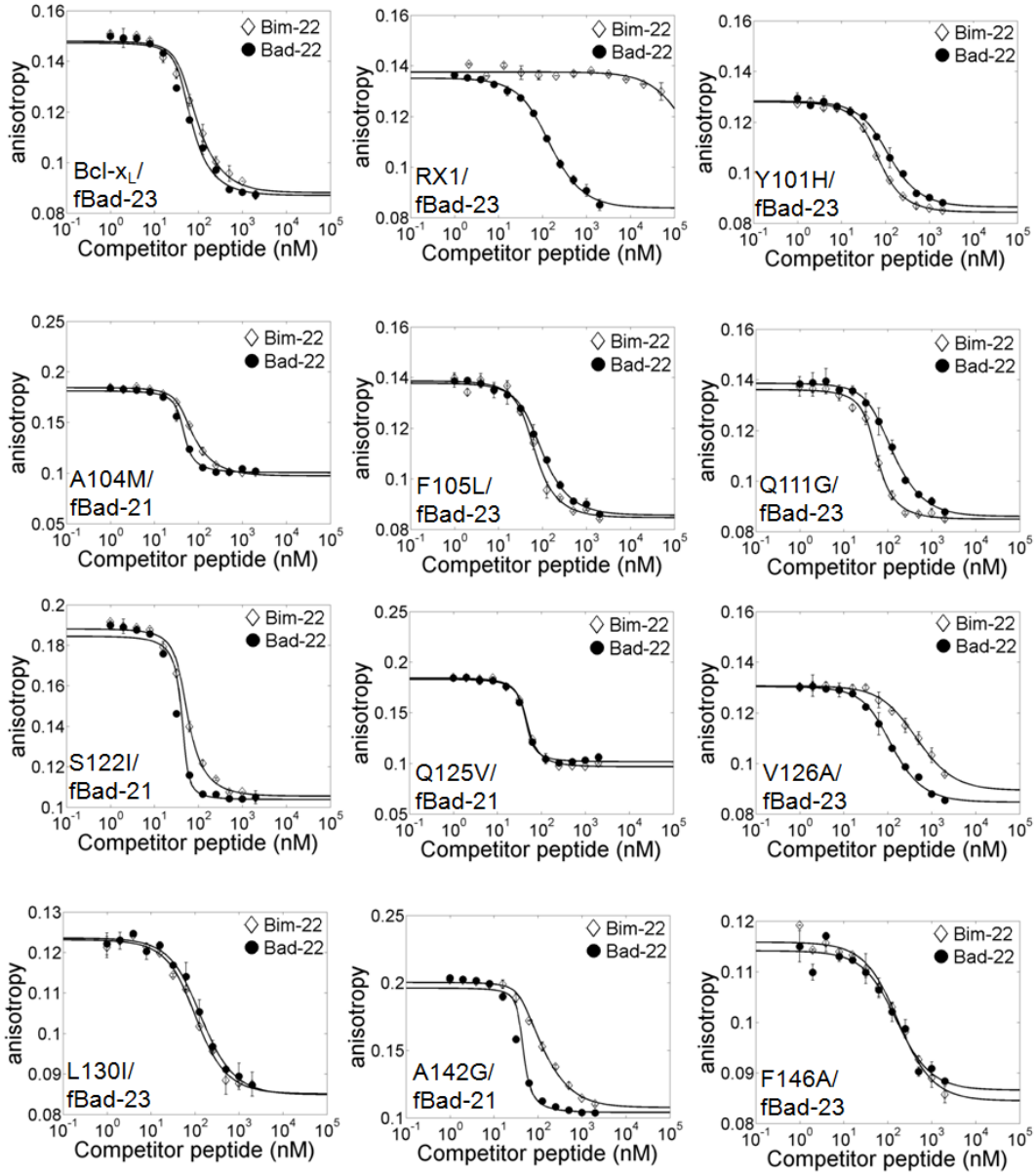
Bim-22
Bad-22
anisotropy
Competitor peptide (nM)
Bcl-xL/ fBad-23
RX1/ fBad-23
Y101H/ fBad-23
A104M/ fBad-21
F105L/ fBad-23
Q111G/ fBad-23
S122I/ fBad-21
Q125V/ fBad-21
V126A/ fBad-23
L130I/ fBad-23
A142G/ fBad-21
F146A/ fBad-23

Figure S5

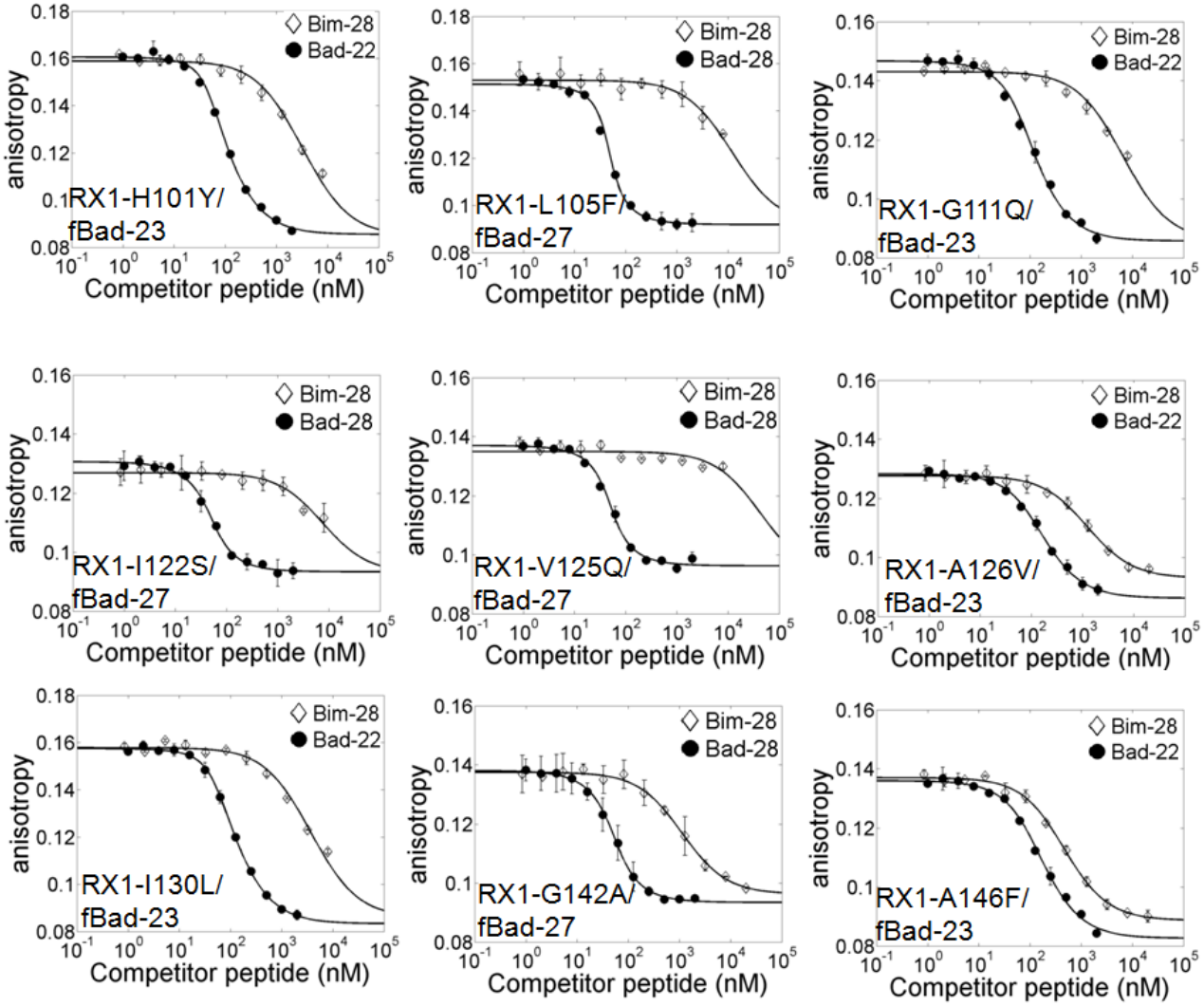
Bim-28
Bad-22
Bad-28
anisotropy
Competitor peptide (nM)
RX1-H101Y/
fBad-23
RX1-L105F/
fBad-27
RX1-G111Q/
fBad-23
RX1-I122S/
fBad-27
RX1-V125Q/
fBad-27
RX1-A126V/
fBad-23
RX1-I130L/
fBad-23
RX1-G142A/
fBad-27
RX1-A146F/
fBad-23

Figure S6

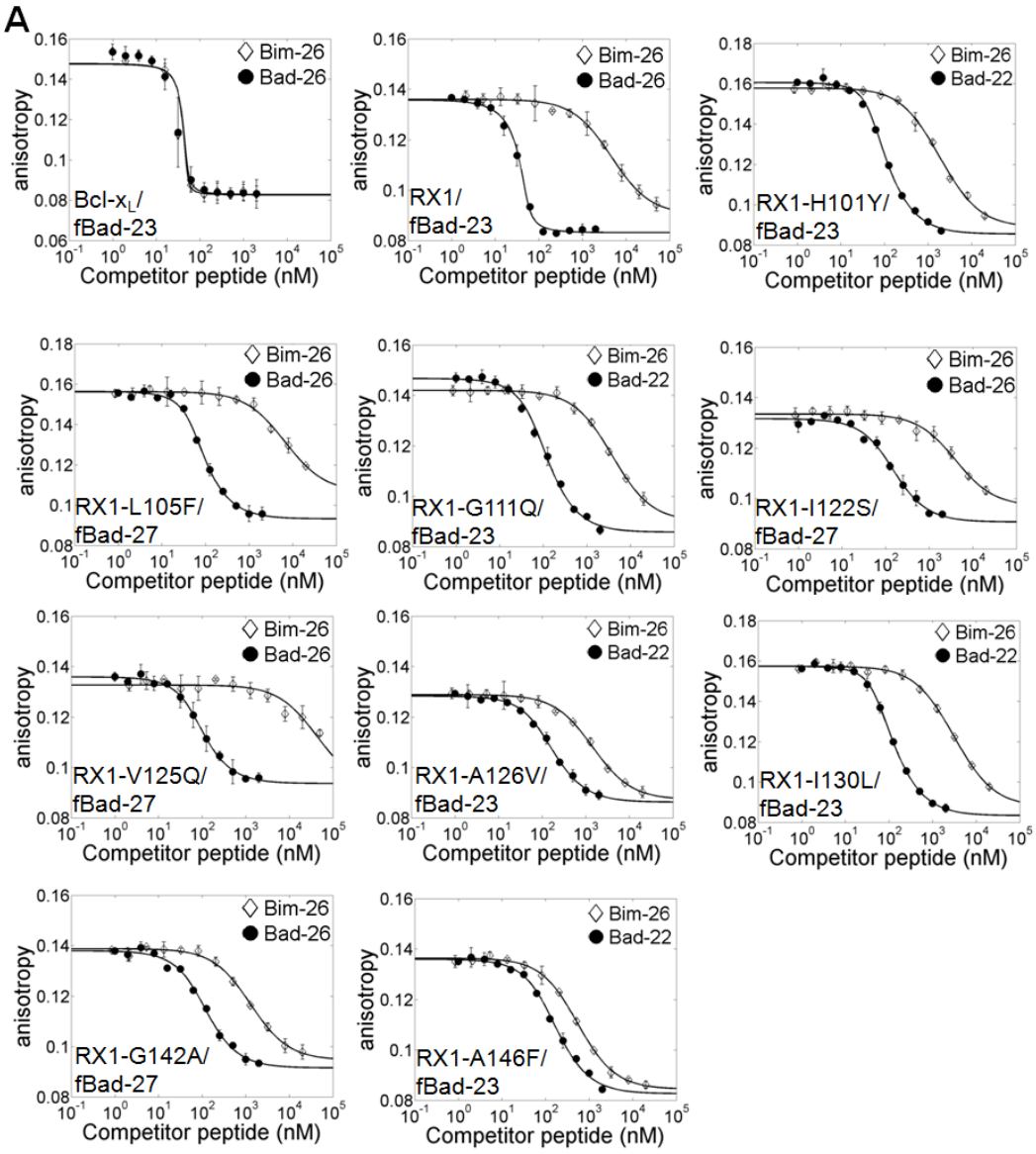
A
Bim-26
Bad-26
Bad-22
anisotropy
Competitor peptide (nM)
Bcl-xL/ fBad-23
RX1/ fBad-23
RX1-H101Y/ fBad-23
RX1-L105F/ fBad-27
RX1-G111Q/ fBad-23
RX1-I122S/ fBad-27
RX1-V125Q/ fBad-27
RX1-A126V/ fBad-23
RX1-I130L/ fBad-23
RX1-G142A/ fBad-27
RX1-A146F/ fBad-23
B
RX1
Kd(Mutant)/Kd(RX1)
Bim
Bad
H101Y
L105F
G111Q
I122S
V125Q
A126V
I130L
G142A
A146F

Figure S7

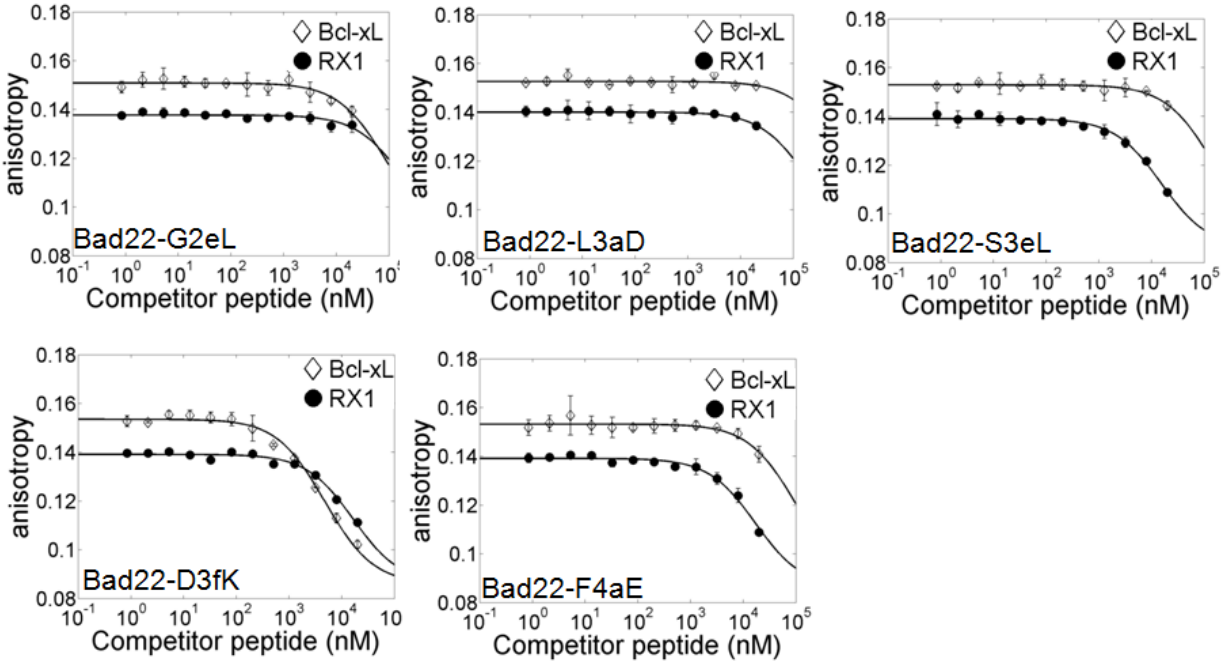
Bcl-xL
RX1
anisotropy
Competitor peptide (nM)
Bad22-G2eL
Bad22-L3aD
Bad22-S3eL
Bad22-D3fK
Bad22-F4aE

Figure S8